Super-hydrophilic properties of TiO$_2$–DLC nanocomposite films fabricated by the simple electrochemical process

Shanhong Wan[a], Liping Wang[a,*], Qunji Xue[a]

[a] State Key Laboratory of Solid Lubrication, Lanzhou Institute of Chemical Physics, Chinese Academy of Sciences, Lanzhou 730000, China

ARTICLE INFO

ABSTRACT

Anatase TiO$_2$ nanoparticles incorporated DLC films were successfully deposited on single crystalline silicon substrates by the electrolysis of TiO$_2$–methanol solution under ambient atmospheric pressure and low temperature. Anatase TiO$_2$ nanoparticles were embedded into amorphous carbon matrix, forming the typical nanocrystalline/amorphous nanocomposite films, confirmed by transmission electron microscopy (TEM). TiO$_2$ incorporation effectively increased the sp^3-hybridized carbon concentration in the composite film, and further regulated the microstructure and surface morphology. Furthermore, the static contact testing completely displayed, TiO$_2$ incorporation got the composite films super-hydrophilic, which fundamentally improved the wetting ability of DLC film.

© 2011 Elsevier B.V. All rights reserved.

1. Introduction

The super-hydrophilic performance of solid-based coatings in possession of anti-fogging, self-cleaning and biocompatibility promised many potential applications in construction industry, mechanical components, optical instruments, and biomedical apparatus, etc. [1]. Diamond-like amorphous carbon (DLC) film versatility demonstrated high hardness, better friction- and wear-resistance, which provided excellently mechanical and tribological behaviors for surface engineering parts. Especially for its good chemical inertness, impermeability and great corrosion-resistance, it guaranteed excellent biological effects of DLC in many key biological and medical devices [2]. However, bad hydrophilic performance in DLC characterized by a higher contact angle of 80° greatly obstacle it as the desired candidates for the corrosion-resistant and biocompatible coatings in clinical applications. In order to further attend biomedical applications, developing antibacterial and biocompatible multi-functional coating was greatly important in the surface engineering of the modern biological and biomedical devices. Previous research showed that, the incorporation of oxygen element into amorphous carbon matrix could regulate the hydrophilic performance of DLC film but did not enhance its bactericidal property, and it highly weakened mechanical properties of DLC film [3]. Accordingly, Thorwarth et al. studied the biocompatible properties of DLC–TiO$_x$ films on TiAl6V4 alloy prepared by the plasma immersion ion implantation and deposi-

tion (PIII&D) technique, and in vitro biocompatibility tests showed promising results concerning the proliferation and differentiation of human osteoblasts for the DLC–TiO$_x$ films [4]. Amin et al. synthesized DLC films containing titanium oxide (DLC–TiO$_x$, $x \leq 2$) using a pulsed DC metal–organic plasma-activated chemical vapor deposition (MOCVD) technique, and they reported that UV light exposure prior to immersion in SBF increased the growth rate of apatite formation significantly as a result of the increased hydrophilicity of the surface [5]. Furthermore, Marciano et al. investigated antibacterial and bacterial activity of DLC coating with and without TiO$_2$ incorporation in detail [6–8], and they pointed out that, as TiO$_2$ content increased, I_D/I_G ratio, hydrogen content and surface roughness increased. Meanwhile, DLC–TiO$_2$ nanocomposite films became more hydrophilic, and the surface energy was higher with the interfacial energy of bacterial adhesion decreasing [7,8]. Absolutely, photo-induced superhydrophilicity of anatase TiO$_2$ displayed good biocompatibility, stability and environmental safety, which have been widely used in the paint industry, biomedicine, electronics and environmental engineering because of its large surface area and sufficient light absorption-ability [1,9]. Thus, the integration of DLC film and anatase TiO$_2$ would be fundamentally significant in surface engineering of biomedical, electronic and environmental applications.

Previous research showed that metal or non-metal doped DLC films have been successfully constructed using the electrochemical process, including F, N, P, and Au [10–13]. Noticeably, the electrochemical method only involved low deposition temperature, simple experimental setup, and easy deposition on substrates with complex shapes. To our knowledge, there was limited work on fabricating TiO$_2$–DLC nanocomposite coating mainly involving

chemical vapor depositing process [4–8] as well as ZnO incorporated DLC film by filtered cathodic vacuum arc (FCVA) technique [14]. Especially, amorphous carbon matrix as the protective coating effectively restrained TiO_2 nanoparticles agglomeration, meanwhile surface properties of DLC was controllably regulated to adapt the biomedical requirement. Therefore, an attempt to deposit anatase TiO_2 nanoparticle incorporated DLC film by the electrochemical method was of great significance in exploiting the new facile fabrication process of novel DLC nanocomposite coating with good wettability.

To achieve the desirable hydrophilic performance of DLC film and further impede TiO_2 nanoparticles agglomeration, an attempt to deposit TiO_2–DLC nanocomposite films was carried out by the simple electro-chemical process at low temperature and ambient atmospheric pressure. Based on the investigation of the surface morphology and microstructure of the obtained films, a possible super-hydrophilic performance of the as-deposited TiO_2–DLC films was interpreted.

2. Experimental details

A simple electrolysis cell system has been described previously [10]. Single crystalline silicon n (1 0 0) with a resistivity of 7–13 Ω/cm² and a size of 30 mm × 10 mm × 0.3 mm was mounted as the negative electrode. The counter-electrode was a graphite plate as the positive electrode, 7 mm away from the negative electrode. Before deposition the silicon substrates were sequentially cleaned by 5%HF acid, deionized water, acetone and ethanol in the ultrasonically bath. The adjustable potential applied to the substrates was 1600 V, the water bath temperature was controlled at 55–60 °C, and the deposition time lasted 10 h. Commercialized anatase TiO_2 nanoparticles with the grain size of 40 nm, were well dispersed into analytically methanol solution with a mass concentration of 0.05 mg/ml. Additionally, DLC films were deposited by the electrolysis of methanol solution for comparison.

The surface morphology of the as-deposited films was observed by CSPM4000 atomic force microscopy (AFM). The chemical composition and bonding states of the samples was characterized by a PerkinElmer PHI-5702 X-ray photoelectron spectroscopy, using Al Kα as the excitation source. Raman spectroscopic measurements were performed on a HR800 Raman spectrometer, operating with an Ar⁺ laser of 532 nm, to investigate the structure of the composite film. The wettability of the samples was characterized by the sessile drop method using a contact angle goniometer (Modle 100-00, Ramé-hart Inc., Mountain Lakes, NJ, USA) to test the contact angle of water.

3. Results and discussions

DLC and TiO_2–DLC nanocomposite films were deposited by the simple electrochemical process under atmospheric pressure and low temperature around 60 °C. Prior to deposition, TiO_2 particles were readily dispersed in methanol solution with a mass concentration of 0.05 mg/ml, and then the mechanical agitator was always operating to maintain TiO_2 homogeneously dispersed in methanol solution during the electrochemical deposition process. For the deposition of pure DLC film, the electric current was about 0.045 A, while it was not greatly changed by the electrolysis of TiO_2–methanol solution, indicating that no additional electrochemical reaction occurred. Therefore, the electrochemical process was speculated following the polarization–dissociation–ionization process [15].

(1) The dissociation of organic precursor of methanol under high electric field between two electrodes.

$$CH_3OH \rightarrow CH_3^{\phi+}OH^{\phi-}$$

$$CH_3^{\phi+}OH^{\phi-} \rightarrow CH_3^+ + OH^-$$
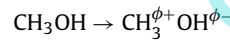
(2) TiO_2 nanoparticles with a higher specific surface would adsorb great amount of cation ions. Under the effect of high electric field, the migration of the cation ions toward to the cathodic substrate with the abundance of electron occurred, resulting in the growth of nc-TiO_2 doped DLC nanocomposite film.

$$mCH_3^+ + nTiO_2 + me^- \rightarrow \text{nc-}TiO_2 \text{ doped DLC nanocomposite film}$$
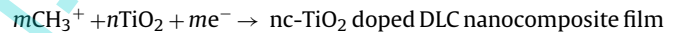
From the above-mentioned process, it was clearly found that nc-TiO_2 doped DLC nanocomposite film was feasibly fabricated under the controllably applied voltage and the mechanical agitator using the simple electrochemical setup. The thickness of the as-deposited films was 800(±50) nm, measured by surface profiler. In contrast with pure DLC film, we firstly systematically investigated the transformation of the surface morphology and the microstructure by the TiO_2 incorporation using AFM, XPS and Raman techniques.

The surface morphology of DLC and TiO_2–DLC nanocomposite films were observed using AFM, shown in Fig. 1. Compared with DLC film, TiO_2–DLC nanocomposite film exhibited a rougher surface with a root-mean-square roughness of 56 nm while 33 nm for DLC films. TiO_2 incorporation possibly disturbed the uniform deposition process, leading to a rougher surface of TiO_2–DLC nanocomposite film. Besides the influence of the electrochemical deposition
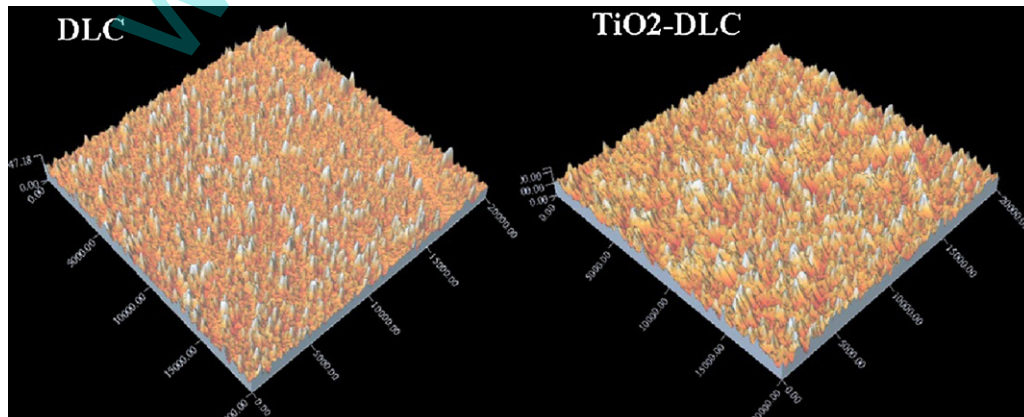

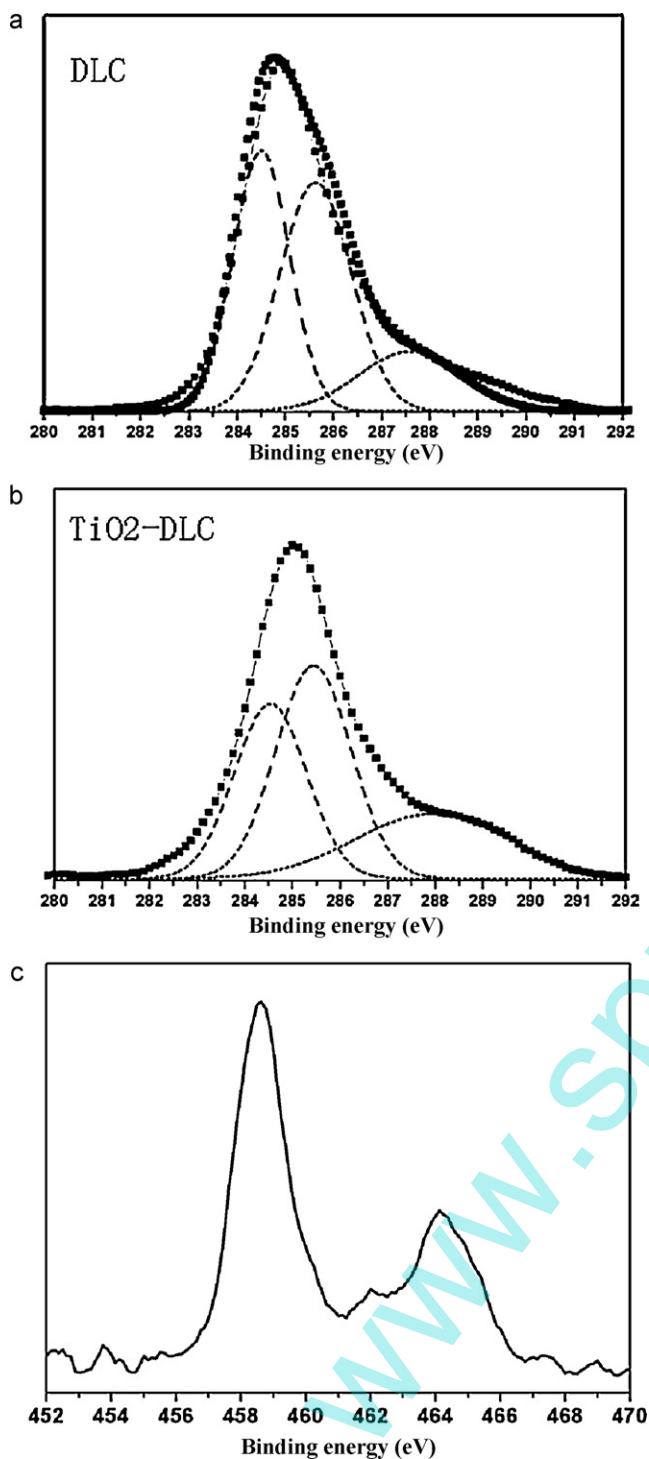**Fig. 1.** AFM images (3D) of DLC film and TiO_2–DLC nanocomposite film.

Fig. 2. XPS analysis: (a) the curve-fitted C1s spectra of DLC and TiO$_2$–DLC film; (b) the spectrum of Ti$_{2p}$ of TiO$_2$–DLC film.

Fig. 3. Raman spectra of DLC and TiO$_2$–DLC films deposited by the electrochemical process.

process itself, surface morphology transformation was also associated with the microstructural change of the films. The chemical composition and bonding state information were characterized by XPS analysis. As shown in Fig. 2, obviously, the C1s spectra were deconvoluted into three peaks: C=C (284.5–284.7 eV), C–C (285.4–285.6 eV) and C–O or C=O (287.5–287.9 eV), and the ratio of sp3/sp2 varied from 1.12 to 1.27. Noticeably, C–O bonds were generally from the surface contamination when exposed to air. For the Ti2p spectrum, the respective position of Ti$_{2p3/2}$ and Ti$_{2p1/2}$ peaks at 458.5 eV and 464.3 eV and the separation of 5.8 eV better indicated
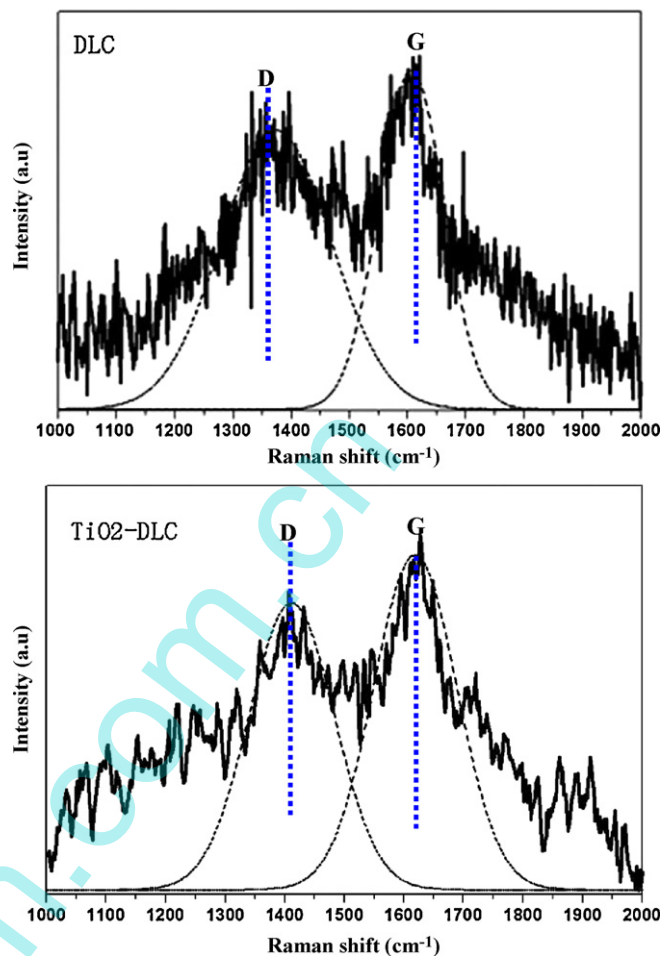
a Ti^{4+} oxidation state [16–18], typical characteristic of anatase TiO$_2$ [19]. Moreover, no indication of a Ti^{3+} emission appeared on the lower binding energy side of the Ti$_{2p}$ signal, which also confirmed anatase phase TiO$_2$ without the rutile phase [20,21]. XPS analysis suggested anatase TiO$_2$ nanoparticles were successfully incorporated into carbon matrix with the Ti/C ratio of 0.031, and TiO$_2$ nanoparticles incorporation effetively improved sp^3-hybridized carbon content. Furthermore, the sp^3/sp^2 ratio could be indirectly deduced from the I_D/I_G ratio in the Raman spectra [2]. Raman spectra could provide enough information to better understand carbon-based materials, typically characterized by the D and G peaks. The D peak dependent on the breathing vibrations of rings at the K-zone boundary corresponded to disordered graphite, while the G peak was related to all sp^2 sites, rings or chains in amorphous carbon films [22]. For the as-obtained films, both D and G peak appeared in DLC and TiO$_2$–DLC film. Raman spectra were further fitted in Guassian mode shown in Fig. 3 and summed up in Table 1. It was shown that a decreased I_D/I_G ratio from 1.38 to 0.87 and the simultaneously downshift of G-peak, as well as the FWHM of D band narrowing. Moreover, Robertson [2] reported that the ratio of I_D/I_G gradually decreased and G-peak down-shifted, indicating the sp^2-hybridized carbon in film decreased. Therefore, TiO$_2$ incorporation effectively enhanced the sp^3-hybridized carbon bonding, which well agreed with XPS analysis. Based on the phenomenological three-stage model developed by Ferrari and Robertson [23,24], when concentration of TiO$_2$ nanoparticles reached the saturation within the DLC film, those particles would separate from the amorphous DLC film. In particular, the grain size of TiO$_2$ nanoparticles

Table 1
The deconvolution band analysis of Raman spectra.

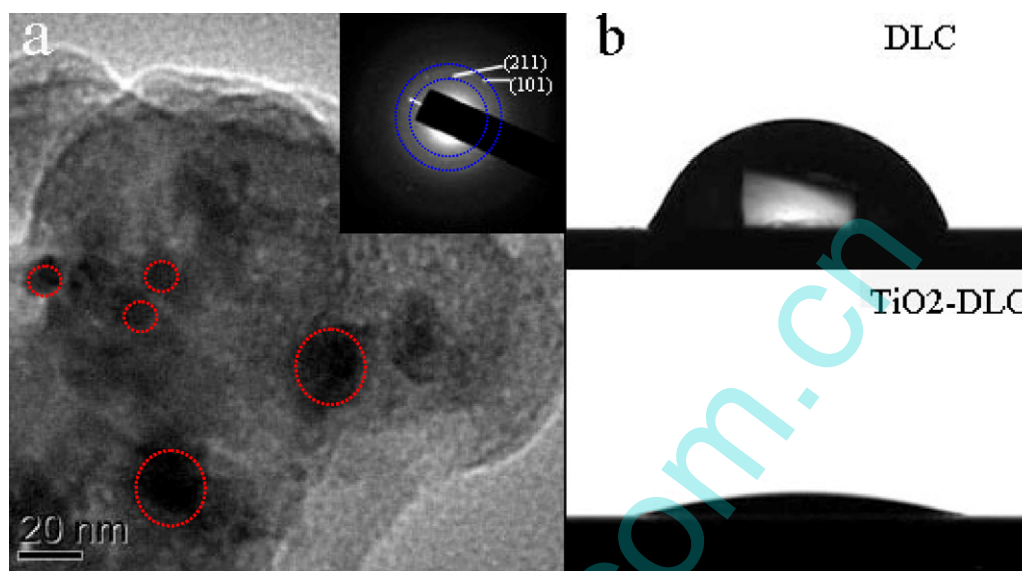| Sample	FWHM of D peak (cm^{-1})	FWHM of G peak (cm^{-1})	I_D/I_G	G peak position (cm^{-1})
DLC	222.5	131.8	1.38	1618
DLC–TiO$_2$	168.5	164.9	0.87	1608

Fig. 4. (a) TEM image of TiO$_2$–DLC nanocomposite film and the corresponding selected area diffraction pattern (the inset); (b) the contact angle of DLC and TiO$_2$–DLC nanocomposite film.

was about 40 nm, theses heteroatoms in amorphous carbon matrix played an important role in the interface widening effect. This factor might make great contributions to the increase of sp^3-hybridized carbon by the incorporation TiO$_2$ nanoparticles in DLC films.

XPS analysis indicated TiO$_2$ particles were incorporated into amorphous carbon matrix, further confirmed by TEM analysis. As shown in Fig. 4a, some TiO$_2$ nanoparticles with a grain size of 40 nm were inhomogeneously embedded in amorphous carbon matrix, which effectively prevented TiO$_2$ nanoparticles from agglomeration. The corresponding selected area electron diffraction (SAED) pattern clearly showed some irregular spot lattices and discrete diffraction rings, indicating anatase crystalline TiO$_2$ nanoclusters with different grain sizes were incorporated into amorphous carbon matrix. Furthermore, the diffraction rings well matched with (1 0 1) and (2 1 1) crystalline planes of anatase TiO$_2$ nanoparticles. Based on the above analysis, anatase TiO$_2$ nanoparticles were successfully incorporated into amorphous carbon matrix without bonding to the ambient carbon atoms, forming the typical nanocrystalline/amorphous matrix structure, and further altered the microstructure of carbon films.

As expected, TiO$_2$–DLC nanocomposite film clearly showed a contact angle of 0–5°, compared with DLC film with a higher contact angle of 80°. It clearly showed DLC film exhibited the super-hydrophilic performance after incorporating anatase TiO$_2$, as shown in Fig. 4b. The wettability of solid surfaces with liquids was strongly dependent on the surface geometry and the chemical composition [25]. Firstly, the surface of the composite film became rougher than that of pure DLC film, which greatly contributed to hydrophilic performance [26]. Also, the chemical composition in the surface was greatly changed by anatase TiO$_2$ nanoparticles inhomogeneously embedded the surface or subsurface, resulting in the enhanced surface energy. As reported, the low contact angle of solids surface had the high surface energy, displaying excellently hydrophilic properties.

Furthermore, anatase TiO$_2$ itself exhibited a hydrophilic properties owing to its photocatalysis [26]. In particular, the band gap of anatase TiO$_2$ might be lowered by the absorbed carbon atoms during the electrochemical process, which would have the positive effect on the improvement of the super-hydrophilic performance of TiO$_2$–DLC nanocomposite film. It also was found TiO$_2$–DLC nanocomposite film exhibited the excellent hydrophilic performance under light irradiation during the testing process. Moreover, the photocatalysis of TiO$_2$ played a part in the super-hydrophilic performance, confirmed by the higher contact angle at night than by day. Ref. [26] reported that the hydrophilic performance of anatase phase TiO2 could be enhanced by carbon doping under visible light irradiation owing to the decrease in the band gap energy. However, the accurate evaluation of the band gap energy and the effect of anatase TiO$_2$ on this hydrophilic performance should be investigated by the further study. In summary, super-hydrophilic performance of TiO$_2$–DLC nanocomposite film greatly explored its potential applications in construction industry, mechanical components, optical instruments, and biomedical apparatus.

4. Conclusions

The fabrication of TiO$_2$–DLC nanocomposite films were successfully performed using the facile electrochemical method under the medium conditions. AnataseTiO$_2$ incorporation effectively made surface rougher, and surprisingly increased the sp^3-hybridized carbon bonding. TiO$_2$–DLC nanocomposite film exhibited the super-hydrophilic performance under the visible light, which strongly depended on the surface geometrical transformation, photo-catalysis of anatase TiO$_2$ and the microstructure alteration. This would widely explore the applications of DLC film from outdoors to indoors. Moreover, this method showed the feasibility for some other metal oxides incorporated into DLC matrix.

Acknowledgement

References

[1] S. Hata, Y. Kai, I. Yamanaka, H. Oosaki, K. Hirota, S. Yamagishi, JSAE Rev. 21 (2000) 97–102.
[2] J. Robertson, Mater. Sci. Eng. R. 37 (2002) 129–281.
[3] S.F. Durrant, R.T.D. Oliveira, S.G.C. Castro, L.E. Bolĺvar-Marínez, D.S. Galväo, J. Vac. Sci. Technol. A 15 (1997) 1334–1339.
[4] G. Thorwarth, B. Saldamli, F. Schwarz, P. Jürgens, C. Leiggener, R. Sader, M. Haeberlen, W. Assmann, B. Stritzker, Plasma Process. Polym. 4 (2007) S364–S368.
[5] M.S. Amin, L.K. Randeniya, A. Bendavid, P.J. Martin, E.W. Preston, Diamond Relat. Mater. 18 (2009) 1139–1144.
[6] F.R. Marciano, D.A. Lima-Oliveira, N.S. Da-Silva, A.V. Diniz, E.J. Corat, V.J. Trava-Airodi, J. Colloid Interface Sci. 340 (2009) 87–92.
[7] F.R. Marciano, L.F. Bonetti, J.F. Mangolin, N.S. Da-Silva, E.J. Corat, V.J. Trava-Airoldi, Vacuum 85 (2011) 662–666.
[8] F.R. Marciano, L.F. Bonetti, N.S. Da-Silva, E.J. Corat, V.J. Trava-Airoldi, Appl. Surf. Sci. 255 (2009) 8377–8382.
[9] Z. Huang, P.C. Maness, D.M. Blake, E.J. Wolfrum, S.L. Smolinski, J. Photochem. Photobiol. A: Chem. 130 (2000) 163–170.
[10] G. Chen, J.Y. Zhang, S.R. Yang, Electrochem. Commun. 10 (2008) 7–11.
[11] S.H. Wan, H.H. Hu, G. Chen, J.Y. Zhang, Electrochem. Commun. 10 (2008) 461–465.
[12] G. Chen, J.Y. Zhang, S.R. Yang, Electrochem. Commun. 9 (2007) 1053–1056.
[13] Q. Fu, C.B. Cao, H.S. Zhu, Mater. Lett. 42 (2000) 166–170.
[14] J. Hsieh, H.C.D. Chua, B.K. Tay, E.H.T. Teo, M. Tanemura, Diamond Relat. Mater. 17 (2008) 167–170.
[15] X.B. Yan, T. Xu, G. Chen, H.W. Liu, S.R. Yang, Carbon 42 (2004) 3103–3108.
[16] K. Bange, C. Ottermann, O. Anderson, U. Jeschowski, Thin Solid Films 197 (1991) 279–285.
[17] W. Gopel, J.A. Anderson, D. Frankel, M. Jaehnig, K. Phillips, J.A. Schafer, G. Rocker, Surf. Sci. 139 (1984) 333–346.
[18] Y. Kagami, T. Yamauchi, Y. Osada, I. Yoshizaura, J. Appl. Phys. 68 (1990) 610–616.
[19] J. F. Moulder, W. F. Stickle, P. E. Sobol, K. D. Bomben, In: J. Chastain (Ed.), Handbook of X-ray Photoelectron Spectroscopy, Second ed., PerkinElmer Corporation, Eden Prairie,Minnesota, 1979.
[20] U. Diebold, Surf. Sci. Rep. 48 (2003) 53–229.
[21] R. Sanjines, H. Tang, H. Berger, F. Gozzo, G. Margaritondo, F. Levy, J. Appl. Phys. 75 (6) (1994) 2945–2951.
[22] F. Tuinstra, J.L. Koening, J. Chem. Phys. 53 (1970) 1126–1130.
[23] A.C. Ferrari, J. Robertson, Phys. Rev. B 61 (2000) 14095–14107.
[24] A.C. Ferrari, J. Robertson, Phys. Rev. B 64 (2001) 075414–075426.
[25] X.J. Feng, L. Jiang, Adv. Mater. 18 (2006) 3063–3078.
[26] H. Irie, S. Washizuka, K. Hashimoto, Thin Solid films 510 (2006) 21–25.